

FSI Analysis of Microcantilevers Vibrating in Fluid Environment

A. Ricci^{1*}, E. Giuri¹

¹ Politecnico di Torino, Materials and Microsystems Laboratory (χ Lab)

*Corresponding author: Palazzo "L. Einaudi", Lungo Piazza D'Armi 6, 10134 Chivasso (To), Italy
alessandro.ricci@polito.it

Abstract: Cantilever vibration in fluid environment is probably one of the most common Fluid Structure Interaction (FSI) problems in the field of Micro/Nano Electro Mechanical Systems (MEMS/NEMS).

Usually the effect of fluid on cantilever oscillation is characterized in terms of mode resonance frequencies and quality factors (Q_s), being those two physical quantities what is actually measured in the dynamic operation.

In this work a new approach to the above FSI problem is proposed: modes Q factors and resonance frequencies in a viscous fluid environment are calculated through an eigenfrequency analysis thus avoiding time domain simulation as in all the previous works about a computational approach to the current problem.

Besides a considerable reduction of the computational time, because of the frequency domain approach, our model demonstrates very high accuracy with respect both to analytical and experimental results.

Keywords: cantilever, FSI, damping, Q factor.

1. Introduction

The oscillation of an elastic structure in a fluid environment probably represents the most typical Fluid-Structure Interaction (FSI) problem.

In the area of Micro Electro-Mechanical Systems (MEMS), such FSI problem is dominated by the presence of fluid viscosity: viscous damping, rather than other damping mechanisms such as acoustic radiation damping or internal structural damping [1], represents indeed the main dissipative process occurring during the oscillation of any microstructure in a fluid environment at ambient or close to ambient, pressures.

Viscosity in the case of MEMS affects both Q factors (Q_s) and resonance frequencies of the vibration modes of the structure, being those two physical quantities what is actually sensed in dynamic measurements.

Cantilever based bio-sensors, currently being probably the most diffuse MEMS devices, should be designed, for instance, so that their mode Q factors are sufficiently high for operation in viscous fluids like water, the natural environment of biology. Their mass sensitivity is indeed directly connected to magnitude of their Q_s thus forcing an accurate design of their geometry to maximize those quantities. To this aim theoretical models for this FSI problem are needed to accurately estimate the fluid effect on Q factors and resonance frequencies.

The aim of this paper is therefore to show a new computational approach to study the effect of a viscous fluid on the mode Q factors and resonance frequencies of a cantilever based device.

It is worth to note that fluid is considered as unconfined therefore leading to the definition of free space damping. Nevertheless our method could be easily extended to simulate also squeeze damping [2], a particular type of fluid-induced dissipation which occurs when a structure vibrates very close to a surface. An example of squeeze film damping simulation is reported at the end of Section 4.

1.1 Brief literature review

Leaving aside those studies in which an analytical approach is combined with a computational one employing home-made numerical codes [3, 4, 5], the literature about a full computational approach to a FSI problem involving cantilevers can be firstly subdivided, according to the problem dimensionality, in two main categories: 2D and 3D simulations.

Refs. [6, 7] contain an example of a bi-dimensional approach: the cantilever is considered long and slender (i.e. $l \gg w$, where l and w are respectively cantilever length and width) so that it is possible to simplify the analysis, restricting the attention to the vibration of the cantilever cross section in a two dimensional fluid domain.

Such an approach, despite of the advantage of being certainly less time-consuming than a three-

dimensional one, becomes less and less accurate with the increase of mode number or the reduction of the beam aspect ratio l/w since, in both cases, fluid flow ceases to possess a genuine 2D nature.

On the other hand, to the second category belong papers [8] and [9] in which the hypothesis about the bi-dimensionality of the fluid flow is relaxed and a fully coupled three-dimensional simulation is performed leading to high accurate results. The analysis of Lee et al. [8] regards nevertheless only the first mode of vibration, while the work of Basak et al. [9], as involving higher harmonics and different mode types represents, to authors knowledge, the most complete work about a full computational approach to the FSI problem above.

What it is worth to stress is that all the papers mentioned so far involve time-domain simulations. The FSI problem is solved by imposing either an initial displacement at the cantilever free end [7, 8] or an initial deformation [9] to the whole beam (in both cases the amplitude of oscillation should be carefully tuned to avoid non-linear effects) and then letting the system evolve over time. If the oscillation is underdamped and cross talk between vibration modes is negligible, the cantilever will behave like a simple damped harmonic oscillator thus experiencing a time decay of the amplitude of vibration. With a further curve fitting step it is possible to evaluate Q factor and resonance frequency of the particular mode under analysis.

1.2 Motivation

The procedure above mentioned suffers from some drawbacks:

I. An initial displacement assigned just to the free end will excite almost only the first mode of vibration (since its shape is the one that mostly conforms to the resultant deformation). On the other hand, imposing to the cantilever an initial deformation proportional to a certain mode shape “in vacuum” [9] (i.e. calculated in a previous undamped eigenfrequency step) is acceptable insofar as the presence of the fluid does not affect that shape. This is strictly true just for the first mode of vibration since its only node¹, being

¹ A node is a point in which the modal displacement equals zero.

located at the clamped end, does not change its position because of the fluid presence. All other higher modes, having nodes located in some position along the beam, are affected by the fluid presence both in terms of frequency and in terms of shape, since the latter fairly depends on node positions. This means that, except for the first mode, setting an initial displacement proportional to an undamped mode shape will produce a damped oscillation in time containing the contribution due to other modes besides the one under analysis fig. 1.

This more and more true with the increase of the fluid damping level, since the effect of damping is to couple all modes of vibration [10]. In other words, even if both the mode shapes in vacuum and in fluid represent a set of orthogonal eigenvectors, the orthogonality is missed when considering one element of the former set respect to the members of the latter. Such modal cross talk complicates the fitting step downstream the time dependent analysis. A Prony analysis [11] is indeed needed to filter the “signal” of the mode under study from the “noise” due to the other modes.

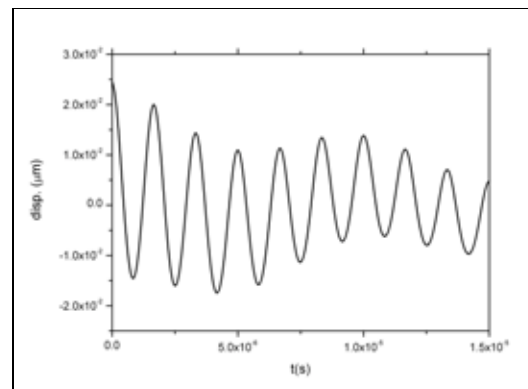


Figure 1. Example of modal cross talk: the time decay of the mode under analysis is affected by the “noise” due to another mode with lower frequency.

II. Time domain simulations are usually highly expensive from a computational point of view. Moreover an accurate convergence study is needed to tune both the time step of the numerical scheme and the stop time of the calculation.

III. The curve fitting step may potentially affect the overall accuracy of the procedure, since the

errors due to the fit are superimposed to the ones due to the computational scheme.

The above drawbacks encourage to move the attention to a frequency domain approach in which mode properties in fluid environment are calculated through an eigenfrequency analysis including damping effects. The benefits of such an approach are evident:

I. On equal mesh density, an eigenfrequency analysis is certainly less time consuming than a time domain one.

II. The convergence study regards just the mesh density and not, as in the time domain approach, both mesh density and time parameters.

III. Mode shapes and frequency in fluid are directly calculated so that no curve fitting step is needed. A possible source of inaccuracy is therefore eliminated.

A damped fully coupled eigenfrequency analysis, on the other hand, is possible only if the equations of Fluid Dynamics could be converted in their frequency domain counterpart. Comsol Multiphysics offers the possibility of enter equations and customize them according to the specific problem under analysis. We exploited this feature in order to modify the standard equations contained in the fluidic module reformulating them as function of frequency.

In this way an FSI eigenfrequency analysis is likely and all the benefits above can be fairly capitalized.

2. Theory and Assumption

When solving a three dimensional FSI problem involving a structure vibrating in a fluid great attention should be paid to contain the overall computational cost of the analysis. The numerical solution of Navier Stokes equations in the three dimensional case certainly represents a challenging task because of both the non-linear nature of such equations and the number of unknowns involved. The computational effort even increases if these equations are coupled to an other set of equations like structural mechanics. Simplifications therefore are not only desired but sometimes also necessary when the computational cost exceeds the computing resources.

Luckily, the FSI problem above presents some features that allow simplifications while virtually preserving the accuracy.

Considering the fluid as incompressible² and neglecting any internal damping in the solid, the problem involves the simultaneous solution of the following set of equations:

$$\nabla \cdot \bar{\sigma} = \rho_s \frac{\partial^2 \bar{u}}{\partial t^2} \quad (1)$$

$$-\nabla p + \mu \nabla^2 \bar{v} - \bar{v} \nabla \bar{v} = \rho_f \frac{\partial \bar{v}}{\partial t} \quad (2a)$$

$$\nabla \cdot \bar{v} = 0 \quad (2b)$$

where $\bar{\sigma}$, ρ_s , \bar{u} , represent stress tensor, density and solid displacement vector, while p , μ , \bar{v} , ρ_f represent pressure, viscosity, fluid velocity vector and density.

If the amplitude of structure vibration is far smaller than any other length scale in the model, eq. (2a) can be linearized [10], i.e. the non-linear convective inertial term $\bar{v} \nabla \bar{v}$ could be dropped thus leading to Stokes equations.

Secondly, by noting that fluid vorticity, defined as $\bar{\omega} = \nabla \times \bar{v}$, plays a significant role just in proximity of the vibrating structure³, it is possible to further simplify Stokes equations in the region of fluid domain sufficiently far from the cantilever.

Setting $\bar{\omega} = \nabla \times \bar{v} = 0$ means that the velocity field satisfies the condition $\bar{v} = \nabla \phi$ where ϕ plays the role of a scalar velocity potential. Substituting the latter expression in eq. (2b) the following equation is obtained:

² Fluid compressibility is significant only when the condition $nL/c \ll 1$, is violated. The quantities n , L , c are respectively the typical frequency of oscillation, the predominant length scale of the solid and the speed of sound in the fluid medium [12]. It is clear that condition above mentioned in the field of MEMS usually holds.

³ Since curl operator involves space derivatives of velocity, the magnitude of these quantities is expected to be high close to the vibrating structure, i.e. where fluid motion is pronounced, and progressively smaller when moving away from it. At an infinite distance from the cantilever, fluid should be indeed at rest.

$$\nabla^2 \phi = 0 \quad (3)$$

On the other hand, using vector identities, eq. (2b) and the irrotational condition above, one has:

$$\nabla^2 \bar{v} = \nabla(\nabla \cdot \bar{v}) - \nabla \times (\nabla \times \bar{v}) = 0 \quad (4)$$

Using again the condition $\bar{v} = \nabla \phi$ and eq. (4), eq. (2a), after having dropped the gradient operator, reduces to the following:

$$p = -\rho_f \frac{\partial \phi}{\partial t} \quad (5)$$

In the region where it is possible to neglect fluid vorticity therefore eqs (2a, b) reduce respectively to eq. (5) and eq. (3). It is worth to notice that these latter equations are uncoupled and therefore pressure can be simply obtained once eq. (3) has been solved.

To sum up, according to distance from the oscillating structure, fluid domain can be subdivided in two parts: a “near field” in which fluid is rotational and therefore eq. (2a) without the $\bar{v} \nabla \bar{v}$ term and eq. (2b) hold and a “far field” in which fluid is irrotational and eqs. (3, 5) hold.

From a numerical point of view, the latter field is far less computationally expensive than the former since the only actual unknown is ϕ , being the pressure variable evaluable downstream the solution of eq. (3).

3. Use of COMSOL Multiphysics

Four Comsol Multiphysics modules were employed for solving the current FSI problem:

- Solid, stress - strain (smsld)
- Stokes (mmglf)
- Laplace equation (irr)
- Moving mesh ALE (ale)

The first two application modes belong to the MEMS module, while the third and the fourth ones are contained respectively in the Comsol Multiphysics PDE modes and Deformed mesh suites. Lastly, for coherence with the above

theoretical treatment, the suffix of the Laplace modules has been changed in “irr” and its dependent variable renamed as “phi”.

The geometry of the model, being symmetrical with respect to xz plane consists of a parallelepiped representing the solid domain (i.e. the cantilever) and two concentric half-spheres representing near and far field of the fluid domain (fig. 2); “smsld”, “mmglf” and “irr” application modes were assigned respectively to the three domains.

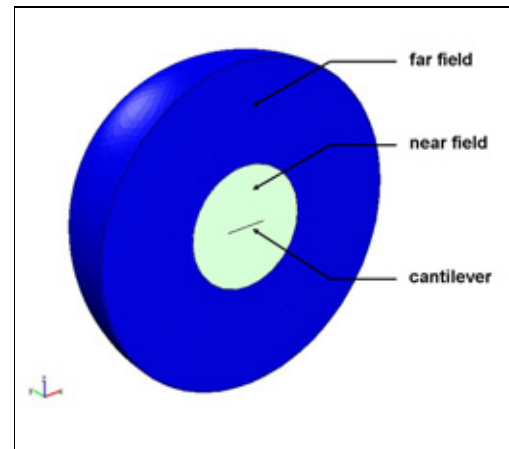


Figure 2. Comsol Multiphysics geometrical model of the current FSI problem.

It is worth to note that the role of the ALE module, in the present model, is noticeably different from the one usually encountered in FSI problems. Moving Mesh application mode is employed just to allow the contraction or expansion of both near and far field fluid domain geometries and meshes and not to account for the modification of the fluid domain shape due to the movement of the solid⁴. Thanks to this module, assigning the first three modules to ALE frame, it is possible, through a preliminary parametric analysis (see Appendix 7.1), to optimize the dimensions of the two fluid domains with respect to ones of the cantilever.

Since all mesh point in the fluid volume are constrained to move without no motion relative to the underlying geometry, ALE module does not affect the overall computational cost.

⁴ According to the Section 2, cantilever is suppose to oscillate in a linear regime. Therefore, the change of the fluid domain shape due to its motion can be neglected.

For what concerns the Solid stress-strain module, the analysis type field was set to “Damped eigenfrequency” so that the variable “*jomega_smsld*” becomes active. For the Stokes module first the transient analysis option was chosen and then the suffix “*t*” for time derivatives was substituted, in the “Equation System” field⁵, with the expression “**jomega_smsld*”.

In this way Stokes equations are converted in the frequency domain and their solution depends on the same frequency parameter of the structural mechanics module.

Finally, in the “Subdomain expression” of the far field subdomain were written both the condition $\bar{v} = \nabla \phi$ and the frequency domain counterpart of eq.(5).

The latter was implemented as:

$$p_{-irr} = -jomega_smsld \cdot \rho_f \cdot \phi \quad (6)$$

The model contains two type of interfaces: solid-near field and near field-far field.

To the first kind of interface, the following boundary conditions were set:

$$\bar{v} = jomega_smsld \cdot \bar{u} \quad (7a)$$

and

$$f^{ext}_smsld = \bar{T}_mmglf \quad (7b)$$

Eq. (7a) belongs to the Stokes module and represents the usual no-slip boundary condition concerning a moving wall, while eq. (7b) is contained in the Structural Mechanics module and states that the total fluid force per unit area acts as external action for the oscillating cantilever.

This last condition, for accuracy reasons, is formulated through Lagrange multipliers [13] enabling non-ideal weak constraints in the Stokes application mode properties.

In correspondence of the second kind of interfaces, the following boundary conditions were set:

$$p = p_{-irr} \quad (8a)$$

⁵ the “Equation system view” in the Model Settings was set to “weak”.

and

$$\frac{\partial \phi}{\partial n} = \bar{v} \cdot \bar{n} \quad (8b)$$

Eq. (8a) is implemented in the Stokes module, while eq. (8b), being \bar{n} the normal unit vector, is the standard Neumann condition for the Laplace equation module.

Since the whole model is symmetrical with respect to *xz* plane (fig. 2), symmetry conditions are required both for the solid and the fluid domains. These are:

$$u_y = 0 \quad (\text{solid}) \quad (9a)$$

$$\begin{cases} v_y = 0 \\ T(x,z) = 0 \end{cases} \quad (\text{fluid near field}) \quad (9b)$$

$$\frac{\partial \phi}{\partial n} = 0 \quad (\text{fluid far field}) \quad (9c)$$

To complete the set of boundary conditions, the clamp boundary condition $\bar{u} = \mathbf{0}$ and the Dirichlet boundary condition are assigned respectively to the fixed end of the cantilever and to the external surface of the fluid far field. The latter, according to eq. (6), mimics an “open” condition since the value of the pressure is constrained to zero.

The equations actually employed by the software are therefore the weak form of the following:

Solid:

$$\nabla \cdot \bar{\sigma} = (jomega_smsld)^2 \cdot \rho_s \bar{u} \quad (10)$$

Fluid near field:

$$\begin{cases} -\nabla p + \mu \nabla^2 \bar{v} = -jomega_smsld \cdot \rho_f \bar{v} \\ \nabla \cdot \bar{v} = 0 \end{cases} \quad (11)$$

Fluid Far Field:

$$\begin{cases} \nabla^2 \phi = 0 \\ p = -jomega_smsld \cdot \rho_f \phi \\ \bar{v} = \nabla \phi \end{cases} \quad (12)$$

The solver simultaneously solves just for the weak forms of eqs. (10), (11) and the first one of eqs. (12) together with the boundary conditions reported above.

Clearly the combination between the frequency domain approach and the simplifications in the physics allow to greatly contain the overall computational cost and simulation time.

3.1 Comsol Multiphysics Simulations

Resonance frequencies and Q factors of the modes of the cantilever vibrating in fluid environment are calculated through an eigenfrequency analysis using the Damped Eigenfrequency solver and Pardiso as linear system solver. Such an analysis occurs “downstream” a preliminary step involving fluid domains optimization (see Appendix 7.1).

After discretization of the equations, being E , D , K , N_F , N respectively the mass, damping, stiffness, constrain force and constrain matrices and U , U_0 the solution vector and the linearization point, the eigensolver solves for the following quadratic eigenvalue problem [13]:

$$\lambda^2 E(U_0)U - \lambda D(U_0)U + K(U_0)U + N_F(U_0)\Lambda = 0 \quad (13)$$

$$N(U_0)U = 0$$

where λ is a complex eigenvalue representing a complex angular frequency.

The resonance frequency and Q factor of each mode in fluid environment are respectively given by:

$$f_{fluid} = \left| \frac{\text{Im}(\lambda)}{2\pi} \right| \quad (14)$$

$$Q_{fluid} = \left| \frac{\text{Im}(\lambda)}{2\text{Re}(\lambda)} \right| \quad (15)$$

Eq.(15) has been implemented in the model as “Global Expression”.

Fig. 3 contains the typical output of an eigenfrequency simulation, i.e., the normalized pressure jump across the cantilever. For each eigenmode, such a quantity is always antisymmetrical with respect to the xy plane.

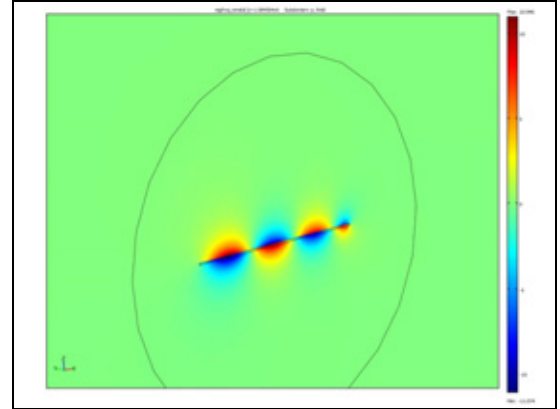


Figure 3. Plot of the normalized pressure jump across the cantilever.

4. Results and discussion

To assess the correctness of our model and the accuracy of the results we analyzed two structures: the first one is cantilever C2 of refs [9, 14], the second one is cantilever A of ref. [15]. While the first one vibrates in a free fluid, the second one oscillates near a surface and squeeze film damping has been showed [15] to dominate its dynamics in moderate vacuum.

Figs. 4 and 5 show the comparison between the available analytical model [16] and our computational results for the first 4 modes of vibration in air environment of cantilever C2.

Such a microstructure is made of crystal silicon⁶, its geometrical dimensions are $l = 197 \mu\text{m}$, $w = 29 \mu\text{m}$, $t = 2 \mu\text{m}$ [9, 14] and its first 4 undamped eigenfrequencies in vacuum, calculated through an eigenfrequency analysis, are 70.90 KHz, 444.16 KHz, 1242.67 KHz, 2433.74 KHz.

Air properties are $\rho = 1.18 \text{ Kg/m}^3$, $\mu = 1.86 \cdot 10^{-5} \text{ Pa}\cdot\text{s}$ [9, 14].

Frequency shifts are calculated as:

$$(f_{fluid} - f_{vac})/f_{vac} \cdot 100.$$

It is worth to note that the analytical model is exact for a beam of infinite length [16] vibrating in an incompressible fluid, even if its predictions are considered sufficiently accurate from aspect ratios l/w higher than 3.5 [16].

A very good agreement between simulation results and analytical data is observed: the maximum deviation between the two set of

⁶ (100) wafer

results is about 6% for frequency shifts and 2.5% for Q factors.

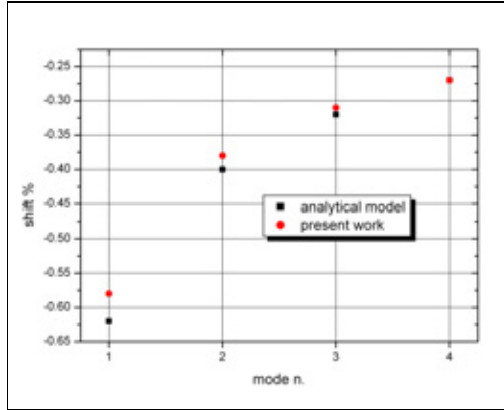


Figure 4. Comparison between analytical [16] and present work results about the frequency shift of the first 4 modes in air environment. The structure under analysis is cantilever C2 of ref. [9, 14].

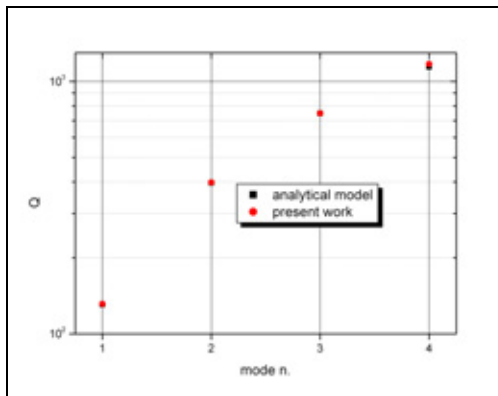


Figure 5. Comparison between analytical [16] and present work results about the Q factors of the first 4 modes in air environment. The structure under analysis is cantilever C2 of ref. [9, 14].

We believe that those deviations are mainly due to the geometrical assumptions in the analytical model. As reported in ref. [17], the error in assuming the cantilever length as infinite decreases with a power law of the mode number. This fact is well pointed out in fig. 4 where analytical data approach simulation results for increasing mode numbers. Other sources of discrepancy could be the unavoidable discretization errors due to the mesh and the fact that the actual implementation of the analytical

model is based on the interpolation of data reported in a tabular form [16].

On the other hand, simulations as well as analytical results shows that fluid viscosity plays a less and less important role as mode number increases. Q values indeed grow with the increase of mode number while frequency shifts decrease with it, approaching the value they would have in an inviscid fluid, where just inertial effect are accounted. More rigorously speaking, the viscous layer thickness, given by $\delta = (2\mu/\rho_f\omega_f)^{0.5}$ where ω_f is the angular frequency of oscillation in fluid, progressively reduces with the increase of mode number, thus reducing the influence of viscosity.

The choice of r (see Appendix 7.1), therefore seems more and more conservative as the mode number increases.

Table 1 (a, b), reports instead a comparison between experimental [9, 14] (“e” superscript), analytical [16] (“a” superscript), and computational (subdivided in the ones of Basak et al. [9], with “B” superscript and the ones of the present work, “pw1,2” superscripts) results. The error is calculated with respect to the experimental values as $(d-e)/e*100$, where d stands for datum and e for the experimental value.

In this case, we performed two types of simulations: in the first one (“pw1” superscript), the cantilever model is simply a parallelepiped rigidly clamped at one end, while in the other one (“pw2” superscript), also a part of the silicon support is modelled⁷ so that the actual stiffness is assigned to the clamp region (fig. 6). In this way simulations are expected to reproduce at best the experimental conditions.

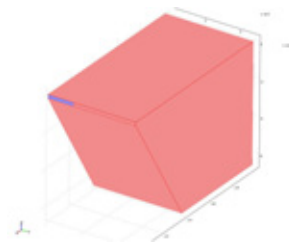


Figure 6. Geometrical Model of the silicon support of cantilever C2 [9, 14]. The clamp area is highlighted in blue.

⁷ The silicon support has been modelled in a separate 3D geometry (fig. 6), clamped at its bottom surface, and linked to the cantilever through “Identity Boundary Conditions”.

Our calculations, in the case in which the effect of the finite stiffness of the clamp is included (“pw2”), shows the smallest errors with respect to the experimental data expect for what concerns the Q factor of the first mode, which has a value slightly lower than the one calculated considering just the cantilever.

On the other hand, both the “pw1” and the “pw2” cases, confirm the high level of accuracy of our computational results.

At last, figs. 7 and 8 show a comparison between the computational results. Our simulations are benchmarked with the ones of Basak et al. [9]. Analytical results [16] are reported as a guide. The fluid considered is water, whose properties are: $\rho = 997 \text{ Kg/m}^3$, $\mu = 8.59 \cdot 10^{-4} \text{ Pa}\cdot\text{s}$ [9, 14].

It is worth to note that while our results and analytical data are quite close to each other (the error never overcomes 5%), the computational results of ref. [9] noticeably differ from them, especially for what concerns frequency ratios (calculated as $f_{\text{fluid}}/f_{\text{vacuum}}$). A likely explanation of this deviation is the fact that, the method followed in ref. [9] involves time domain simulations which suffer from some drawbacks. As explained indeed in the Subsection 1.2, such type of simulations requires a post-processing step of results in which the curve “displacement vs. time”, obtained from the simulations, is fitted to a damped sinusoid. When the structure vibrates in a highly viscous fluid like water, the

damping level could be so high that all modes are sensibly coupled and a Prony analysis [11] of results is needed to separate the signal of a particular mode from the noise due to the others. It follows that a simple fit with a damped sinusoid, as the one employed by Basak et al. [9], is not satisfying in those cases.

Tabs. 2 (a, b) show, instead, the comparison between experimental [15], analytical [18] and computational results about cantilever A [15]. This is an electrostatically actuated crystal silicon microbeam vibrating close to a surface which, in turn, works as counter-electrode. Geometrical average dimensions are: $l = 495 \mu\text{m}$, $w = 35 \mu\text{m}$, $t = 3.3 \mu\text{m}$ and $g_0 = 6.45 \mu\text{m}$, where g_0 represents the static gap height between the cantilever and the electrode. Air temperature is considered to be 20°C .

Since squeeze film damping has been showed to be the predominant damping mechanism in the molecular regime [15], we decided to employ also the Comsol Multiphysics application mode “Solid, stress-strain with film Damping”, belonging to the MEMS module, and verify its predictions by realizing a dedicated model. This last consists of a parallelepiped clamped at one end and having squeeze film damping equations assigned to one of the its surfaces of area $l \cdot w$. All other surfaces are considered as free.

mode n.	f^e		f^a		f^B		f^{pw1}		f^{pw2}	
	data (KHz)	err%								
1	69.87	-	70.61	1.06	70.49	0.89	70.49	0.89	69.52	-0.50
2	438.5	-	443.50	1.14	441.6	0.71	442.45	0.90	436.23	-0.52

Table 1a. Comparison between experimental (e) [9, 14], analytical (a) [16] and computational (B “Basak et al. [9]”, pw1, 2 “present work”) results about the first two mode resonance frequencies in air environment of cantilever C2 [9, 14].

mode n.	Q^e		Q^a		Q^B		Q^{pw1}		Q^{pw2}	
	data	err%	data	err%	data	err%	data	err%	data	err%
1	136	-	130.7	-3.89	144.8	6.47	131.4	-3.38	130.4	-4.12
2	395	-	396.8	0.45	367	-7.09	397.7	0.68	394.4	-0.15

Table 1b. Comparison between experimental (e) [9, 14], analytical (a) [16] and computational (B “Basak et al. [9]”, pw1, 2 “present work”) results about the first two mode Q factors in air environment of cantilever C2 [9, 14].

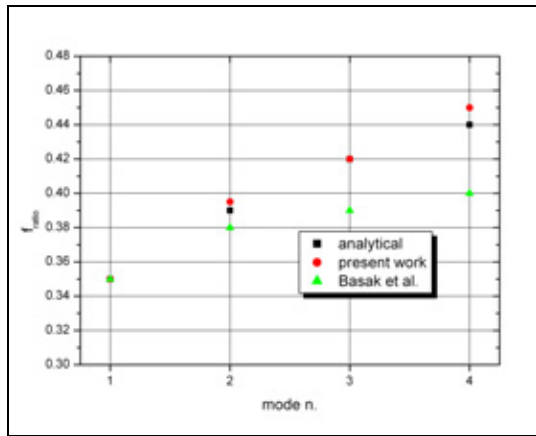


Figure 7. Comparison between analytical [16], present work and Basak et al. [9] results about frequency ratios (calculated as f_{fluid}/f_{vacuum}) for the first four mode of cantilever C2 in water environment [9, 14].

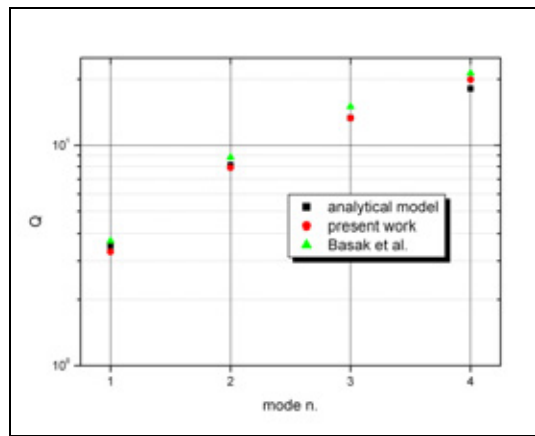


Figure 8. Comparison between analytical [16], present work and Basak et al. [9] results for the first four mode Q factors of cantilever C2 in water environment [9, 14].

On the other hand, the complete FSI model has been obtained positioning the cantilever at a distance g_0 from a surface to which wall boundary conditions⁸ were assigned (fig. 9).

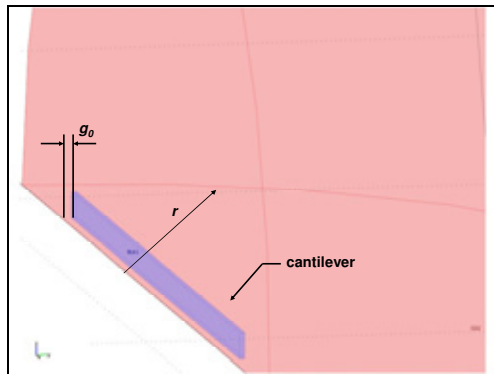


Figure 9. Detail of the 3D FSI model about a cantilever vibrating near a surface at distance g_0 [15]. Only the near field is showed.

Tab. 2a contains the results about first mode resonance frequencies, while tab. 2b the calculated values of Q factors. Superscripts “s1” and “s2” refer respectively to the full 3D FSI

computational model and the simplified squeeze film damping model.

Tab. 2a shows that both the analytical model and the full 3D FSI computational model fail to predict the actual frequency shift, even if the agreement between them is a quite good. This is due to the fact that the experimental frequency shift is due to a superposition of the damping and “spring softening” effects, being the latter a phenomenon which occurs in electrostatically actuated microstructures [15].

In Tab. 2b, on the contrary, is showed that the experimental Q factor, being far less affected by electrostatic effects, shows a good agreement both with the analytical model and our computational ones, even if the latter seem to be more accurate.

For what concerns the squeeze film damping simulation, both Tabs. 2a and 2b put in evidence that such a model greatly underestimates the effect of fluid on the resonance properties: frequency shift and Q factor values appear to be the former about half and the latter about two times the other corresponding theoretical values. This means that, whenever viscosity effects are predominant (i.e. when fluid pressure has a value close to the ambient one) the squeeze film damping model is not appropriate to describe such an experimental case.

⁸ Wall boundary condition for the far field portion of the fluid domain regards only the normal component of velocity and therefore it is equal to eq. 9c.

f_{vac}^e	$shift_{air}^e$	f_{vac}^a		$shift_{air}^a$		f_{vac}^{s1}		$shift_{air}^{s1}$		$shift_{air}^{s2}$	
data (KHz)	data	data (KHz)	err %	data	err %	data (KHz)	err %	data	err %	data	err %
18.33	-2.10	18.45	0.68	-0.74	-64.91	18.54	1.16	-1.00	-52.42	-0.07	-96.67

Table 2a. Comparison between experimental (e) [15], analytical (a) [18] and computational results (subdivided in the ones calculates through the full 3D FSI model, “s1” superscript, and those obtained by the “Solid, stress-strain with film Damping” application mode, “s2” superscript) about the first mode resonance frequency of cantilever A [15].

Q_{air}^e	Q_{air}^a		Q_{air}^{s1}		Q_{air}^{s2}	
	data	err %	data	err %	data	err %
5.7	6.0	5.1	5.5	-3.0	12.7	123.81

Table 2b. Comparison between experimental (e) [15], analytical (a) [18] and computational results (subdivided in the ones calculates through the full 3D FSI model, “s1” superscript, and those obtained by the “Solid, stress-strain with film Damping” application mode, “s2” superscript) about the first mode Q factor of cantilever A [15].

For instance, this simplified model does not take in account the presence of the unbounded fluid on the other side of the cantilever, which certainly plays a role in the actual device operation within the viscous regime.

5. Conclusions

In this work a new approach to a FSI analysis of microcantilevers vibrating in fluid environment has been proposed. Modes Q factors and resonance frequencies in a viscous fluid are calculated through an eigenfrequency analysis thus avoiding time domain simulation. The frequency domain approach, combined with the subdivision of the fluid domain in a viscous and irrotational part, leads both to a strong reduction of the computational cost with respect to the time domain approach and to a high degree of accuracy of the results, as shown by the benchmark with available analytical and experimental data.

We can conclude therefore that our FSI model appears to work in a very general context, being suitable also for those cases in which, even if there is a surface in proximity of the vibrating structure, the squeeze film damping model fails.

6. References

1. R. Lifshitz, M. L. Roukes, *Thermoelastic damping in micro- and nanomechanical systems*, Phys. Rev. B, **61**, 5600-5609 (2000).
2. M. Bao, *Squeeze film air damping in MEMS*, Sens. Act. A, **136**, 3-27 (2007).
3. E. O. Tuck, *Calculation of unsteady flows due to small motion of cylinders in a viscous fluid*, J Eng. Math, **3**, 29-44 (1969)
4. Y. Kerboua, A.A. Lakis, M. Thomas, L. Marcouiller, *Vibration analysis of rectangular plates coupled with fluid*, Appl. Math. Mod., **32**, 2570–2586 (2008).
5. Weiss, K. Reichel, Jakoby, *Modeling of a clamped-clamped beam vibrating in a fluid for viscosity and density sensing regarding compressibility*, Sens. Act. A., **143**, 293–301 (2008).
6. W. Zhang, M. Requa, K. Turner, *Determination of Frequency Dependent Fluid Damping of Micro and Nano Resonators for Different Cross-Sections*, Nanotech 2006, Boston, MA May (2006)
7. W. Zhang, K. Turner, *Frequency dependent fluid damping of micro/nano flexural resonators: Experiment, model and analysis*, Sens. Act. A, **134**, 594–599 (2007).
8. J. H. Lee, S. T. Lee, C. M. Yao, W. Fang, *Comments on the size effect on the microcantilever quality factor in free air space*, J. Micromech. Microeng., **17**, 139–146 (2007).
9. S. Basak, A. Raman, *Hydrodynamic loading of microcantilevers vibrating in viscous fluids*, J. Appl. Phys, **99**, 114906 (2006).
10. J. E. Sader, *Frequency response of cantilever beams immersed in viscous fluids with applications to the atomic force microscope*, J. Appl. Phys., **84**, 64-76 (1998).
11. http://en.wikipedia.org/wiki/Prony's_method

12. G.K. Batchelor, *An Introduction to Fluid Dynamics*, **169**, Cambridge University Press, Cambridge (1967).
13. Comsol Multiphysics 3.5a Manuals
14. J. W. M. Chon, P. Mulvaney, J. E. Sader, *Experimental validation of theoretical models for the frequency response of atomic force microscope cantilever beams immersed in fluids*, *J. Appl. Phys.*, **87**, 3978-3988 (2000).
15. Cocuzza et al., *Silicon laterally resonant microcantilevers for absolute pressure measurement with integrated actuation and readout*, *J. Vac. Sci. Technol. B*, **26**, 1071-1023 (2008).
16. C. A. Van Eysden, J. E. Sader, *Frequency response of cantilever beams immersed in viscous fluids with applications to the atomic force microscope: Arbitrary mode order*, *J. Appl. Phys.*, **101**, 044908 (2007).
17. F. J. Elmer, M. Dreier, *Eigenfrequencies of a rectangular atomic force microscope cantilever in a medium*, *J. Appl. Phys.* **81**, 7709 -7714 (1997).
18. C. P. Green, J. E. Sader, *Frequency response of cantilever beams immersed in viscous fluids near a solid surface with applications to the atomic force microscope*, *J. Appl. Phys.* **98**, 114913 (2005).

7. Appendix

7.1 Parametric Analysis

Before the eigenfrequency solution step, a parametric analysis involving also the ALE application mode and with the aim of scaling the geometry of the fluid domains, has been performed.

The scaling has been enforced by means of a subdomain condition in the ALE module where domains contraction or expansion are function of a parameter called “disp”.

By combining in a sequence, through the Solver Manager, the static and the eigenfrequency steps in a parametric sweep as function of “disp” parameter, it has been possible to study the variation of Q factors and resonant frequencies with respect to the change of the radius of both the near (r) and far field (R) fluid domain. The change of former allows to evaluate at what distance away from the cantilever, fluid can be considered as fairly irrotational, while by changing the latter, it is possible to evaluate the

effect on results of the finite size of the fluid domain.

Results were accepted whenever the following condition was satisfied:

$$\left| \frac{A_1 - A_0}{A_0} \right| \leq 0.01 \quad (16)$$

where A can represent both Q factor and resonance frequency of the mode under analysis and subscripts 0 and 1 are referred respectively to the “base” value of r or R and to a larger value of them.

It was found that the conditions $r \geq 1.1l$ and $R \geq 3l$ assure geometry-independent results, provided that the mesh is sufficiently dense. It is worth to note the first condition corresponds to $r \approx O(10\delta)$ which implies that viscous effects are accurately captured.

Mesh density has been in turn tuned first checking the convergence of the mode frequencies in vacuum (eq. (17) was employed) and then setting a value of 1.27 in the field “Element Grow Rate” in the mesh subdomain settings for both the fluid domains.

The resulting mesh, in the free fluid case, has a total number of elements which is about 35000, which corresponds to a total number of d.o.f. of about 170000.